CO_2 SOIL FLUX IN TEMPERATE FORESTS LOCATED IN SOUTHERN ONTARIO

By Bronwyn Riddoch

A Thesis

Submitted to the School of Interdisciplinary Science

In Partial Fulfilment of the Requirements

of the Degree

Bachelor of
Science

McMaster University

BACHELOR OF SCIENCE (2022) McMaster University

School of Interdisciplinary Science Hamilton, Ontario

TITLE: CO_2 Soil Flux in Temperate Forests Located in Southern Ontario

AUTHOR: Bronwyn Riddoch

SUPERVISOR: Dr. M. Altaf Arain

NUMBER OF PAGES: vii, 34

Abstract

Forests sequester large amounts of CO_2 from the atmosphere, playing a significant role in the global carbon cycle and contributing significantly to building carbon sinks. Some of the sequestered carbon is released back into the atmosphere through autotrophic and heterotrophic respiration. The release of carbon, known as soil respiration (Rs), is regulated by environmental factors, primarily soil temperature (Ts) and soil moisture (SM). This study examines the difference in Rs at two forests sites in Southern Ontario for the 2021 growing season using automated CO_2 flux measurement systems. The first site is a mature coniferous forest (TP74), and the second is a mature deciduous forest (TPD). There was no clear relationship between Rs and Ts or SM at both sites, primarily due to limited observed data available in 2021. However, it was found that an increase in SM could cause a different Rs response between the sites. When both sites experienced an increase in SM, on the same day, Rs increased at TPD, but Rs decreased at TP74. The difference in the response may be due to differences in organic material between sites, with TPD having a higher amount of organic material. A Rs Ts SM model was fitted to the data, but the correlation was poor at both sites. Model parameters from a past study at TPD were used to simulate Rs at TPD for whole year. These findings contribute to the understanding of Rs in different forest types and how environmental factors may alter rates of Rs.

Acknowledgements

I would like to thank my supervisor, Dr. Altaf Arain, for giving me the opportunity to learn under his supervision. His knowledge and patience has been instrumental in helping me navigate my first years in scientific research and to grow as a student. I am truly grateful for the opportunity to work with him. Thank you to everyone in the Hydrometeorology and Climatology Group for the data collection and for answering all of my questions. Thank you to the project funders NSERC and Global Water Future Program. Thank you for the in-kind support from OMNFR, SWCRCC and LRPCA.

I would also like to thank my grandparents, parents, aunts, and siblings. Thank you for your support, guidance, love, and countless proof readings. Lastly, special thanks to Scott Darlington for connecting me with Dr. Arain.

Table of Contents

List of Tables

List of Figures

Introduction

Through photosynthesis and evapotranspiration, forests sequester large amounts of CO_2 from the atmosphere. This process plays a significant role in the global carbon and water cycles and contributes to creating significant carbon sinks within forests (Beamesderfer et al., 2020). Some sequestered CO_2 is released back into the atmosphere through autotrophic respiration, while the remaining CO_2 is released through heterotrophic respiration. Annually, this exchange amounts to 120 gigatons of carbon released into the atmosphere and is the second-largest carbon flux connecting the atmosphere and terrestrial biospheres (Hibbard et al., 2005; Yuste et al., 2005; Giasson et al., 2013). The release of carbon through autotrophic and heterotrophic respiration is referred to as soil respiration (Rs) (Liu et al., 2019).

Carbon released into the atmosphere from forest root activity is known as autotrophic respiration (Wei, Weile and Shaopeng, 2010). When identifying the carbon sources within autotrophic respiration, autotrophic respiration can be broken down further into two categories; growth respiration and maintenance respiration (Piao et al., 2010). Studies typically account for the effect of plant biomass, age, nutrients, and temperature on autotropic respiration (Ryan, 1991; Piao et al., 2010). Heterotopic respiration is defined as the carbon released from the microbial decomposition of organic materials (Tang et al., 2020). Current research suggests that temperature, moisture and organic matter input into the soil system are the driving factors in heterotopic respiration rates (Bond-Lamberty et al., 2018). Many studies have shown that the primary controlling factor on autotrophic and heterotopic respiration is soil temperature (Ts), followed by soil moisture (SM) (Borken et al., 2002; Hibbard et al., 2005; Giasson et al., 2013; Bhanja and Wang, 2021; Klimek, Chodak and Niklińska, 2021).

Rs rates are also dependant on the vegetation. Giasson et al. (2013) found that vegetation phenology influences soil Rs. They demonstrate that there are clear inter-annual variations within the observed Rs rates (Giasson et al., 2013). These patterns can be tied to plant growth and activity stage, with less activity correlating to lower Rs rates (Huang, Gu and Niu, 2014). In addition, differences in Rs rates can be seen in different forest types, regardless of environmental factors (Borken et al., 2002; Klimek, Chodak and Niklińska, 2021). Soil characteristics, including soil C: N ratio, dissolved organic carbon, and soil pH, all have a strong effect on Rs and often are determined by forest type (Klimek, Chodak and Niklińska, 2021).

It is undisputed that climate change not only affects Rs rates but also soil-carbon dynamics as a whole (Bradford et al., 2016; Johnston and Sibly, 2018). Studies have shown that the warming associated with climate change has stimulated heterotopic respiration, the biological component of Rs. Wallenstein et al. (2011) have found that the accelerated heterotopic respiration in warm temperatures is due to increased activity in extracellular enzymes that degrade polymeric organic matter in the soil. This increase in activity of the microbes accelerates the decomposition rate of soil carbon to CO_2, resulting in increased Rs and creating a positive feedback loop (Bradford et al., 2016; Johnston and Sibly, 2018; Lei et al., 2021). The increase of soil decomposition will limit the ability of the land to be a carbon sink and will lead to an increase of the anthropogenetic CO_2 remaining in the atmosphere, thus affecting planetary warming (Bradford et al., 2016).

Not only is the expected warming temperatures associated with climate change worrying for Rs rates, so too are the extreme weather events. Events of concern include: warmer spring temperatures, intense heat and drought in summer, large precipitation events, reduced snowfall and early snowmelt in the winter (Bonan, 2008; Allen et al., 2010; Teskey et al., 2015; Beamesderfer et al., 2020). After significant precipitation events, large fluxes occur in Rs rates and account for the majority of the annual soil CO_2 efflux (Song, Niu and Wan, 2016; Smith et al., 2017; Liu et al., 2019). Various physical, chemical and biological mechanisms contribute to the influx of Rs after the precipitation events (Unger et al., 2010; Liu et al., 2019). CO_2 gas that has accumulated in the dry period displaced by rainwater infiltrating into the soil pores after a precipitation event (Yan et al., 2014; Liu et al., 2019). This interaction releases the soil CO_2 back into the atmosphere, because the soil is unable to store both the gas and the water (Yan et al., 2014; Liu et al., 2019).

The increase in Rs after a precipitation event is also related to the population and activity of the soil microbial community (Orchard and Cook, 1983; Unger et al., 2010; Yan et al., 2014; Liu et al., 2019). After a precipitation event, the additional moisture content within the soil increases the fungal and microbial biomass in response to increased water availability (Unger et al., 2010; Liu et al., 2019). The movement of nutrients facilitated by rainfall leads to an increase in fungal and microbial biomass and to the activity of the community (Orchard and Cook, 1983; Yan et al., 2014). Together, these responses combine to increase the biomass and to the activity of the fungal and microbial community, resulting in an increase in heterotopic respiration and translating into greater Rs rates (Orchard and Cook, 1983; Unger et al., 2010; Yan et al., 2014; Liu et al., 2019).

The main objective of this study is to gain insight into soil CO_2 emissions in a deciduous and coniferous forest in the Great Lakes region. The specific aims of this study are to: (1) to measure

CO_2 efflux within a coniferous (TP74) and deciduous (TPD) forest ecosystem using automated soil chambers; (2) determine the impacts of environmental variables and extreme weather events on soil respiration in both forests; and (3) develop and examine the soil respiration models in simulating soil respiration in these forest ecosystems.

Methods

Site Descriptions

Two sites were investigated in this study, both located on the north shore of Lake Erie in Southern Ontario, Canada (42˚ 71′ N, 80˚ 35′ W). Both are part of the Turkey Point Flux Station and are within 20 km of each other. One site was established in 1974 and is a 47-year-old mature coniferous forest, from here on known as TP74 (Turkey Point 1974). The other site was established in the early 1900s and is approximately a 90-year-old mature deciduous forest, from here on known as TPD (Turkey Point Deciduous). TP74 is a monocultural, primarily of eastern white pine (*Pinus strobus L.),* although 5% of the tree species are Jack pine (*Pinus banksiana)* and 1% are oak. TPD is far more diverse, with the predominate tree species including white oak (*Quercus alba*), sugar and red maple (*Acer saccharum*, *A. rubarum*), American beech (*Facus grandifolia*), red oak (*Q. veluntia*, *Q. rubra*), and white ash (*Fraxinus Americana*). The soil is very similar within the two sites. TP74 soil is 98% sand, 1% silt, and <1% clay, where TPD soil is over 90% sand. Both sites are well-drained.

Soil and Ecosystem Measurements

At both sites, Rs measurements were recorded in continuous half-hour intervals from April 2021 to December 2021 using an automated CO_2 flux measurement system affixed to permanent collars. The measurement equipment contains three main components: the gas analyzer (LI-

8100A), long-term measurement chambers (LI 8100-104), a multiplexer for multiple chamber measurements (LI-8150). Each chamber is located 15 m from the measurement equipment with Ts and SM probes (LI-8150 – 203 and GS-1, respectively) buried at 5 cm located outside the collar. The soil collars are PVC pipe with a diameter of 20 cm, a thickness of 1 cm, and a height of 11.5 cm. The collars are exposed 3 cm above the surface, with the remaining 8 cm inserted into the soil. Further details are provided in Daly (2016) and Ma (2020). Three and five chambers are deployed at TP74 and TPD, respectively.

An automatic weather station (Campbell Scientific Inc), part of a closed-path eddy covariance system at each site, was used to gather metrological data. Instruments in the closed-path eddy covariance system are installed above the canopy at 36 m high and affixed to the top of a scaffolding tower. The metrological data was sampled every five seconds and averaged half-hourly using a data logger (CR3000, CSI). Net radiation (Rn) measurements were collected using four dome net radiometers (CNR4, Kipp and Zonen). Air temperature (Ta) and relative humidity (HMP155A, CSI) were also collected on the tower. Ts and SM were measured for the same time period in two locations, known as the soil pits, at both sites, near the eddy covariance flux tower and CO_2 chamber locations. Measurement readings at the soil pits for Ts and SM were made at 2, 5, 10, 20, 50, 100 cm depths at each location. Further details of flux, meteorological, and soil data measurements are provided in Beamesderfer et al. (2020).

Commencement of data analysis found that the automated CO_2 flux measurement system experienced collection errors for the first half of the season, and no valid data was collected at either site from April to July. As such, this study will only be looking at Rs data from the latter half of the 2021 growing season, from August to October. For the August to October timeframe, there were two functioning chambers at TPD and one functioning chamber at TP74. Additionally, the Ts and SM probes attached to the automated CO_2 flux measurement system malfunctioned for the 2021 growing season. Thus, average 5 cm Ts and SM data from the soil pits have been substituted at TPD. However, the Ts probes at the TP74 soil pits also malfunctioned. Only SM data is available at TP74 for the 2021 growing season as Ts data is not available for TP74 for the available Rs data. In a nearby study forest of eastern white pine (*P. strobus L.),* known as TP39 (Turkey Point 1939), the Ts probes in the soil pits collected data until August 31st, 2021. Average 5 cm TP39 Ts data has been used to replace the missing TP74 Ts data. In some scenarios, Ta readings from TP74 have been substituted for TP74 Ts data. In other cases, if data past August 31st was needed, Ts data from TPD was used instead of TP39 Ts data to replace TP74 Ts data. Figure 1 shows the regression fit between available TP39 and TPD 5 cm Ts data. Every substitution is noted throughout the results section.

Data Analysis and Modeling

Soil CO_2 emissions data was processed using Soil Flux Pro software (4.0.1; Li-COR Inc.). Rn, Ts, SM, Ta, and Rs data were imported into MATLAB (2020b; MATLAB) for analyses and trend exploration. 30-minute interval Rs data below 0 µmol CO2 $m^{-2}s^{-1}$ or above 20 µmol CO2 $m^{-2}s^{-1}$ was removed from the data set. 30-minute interval Ts, SM, Ta, and Rs data was used to create plots to show daily trends. Other times, 30-minute interval Ts, SM, Ta, and Rs data were averaged to produce daily means.

To create the model, the parameters *a* and *b* had to be derived. A classic parametric exponential model, as seen in Equation 1, was used to describe the relationship between Rs and Ts at both sites:

$$y = ae^{bT} \tag{1}$$

where *y* is measured Rs rate, *T* is the measured Ts at 5 cm, and *a* and *b* are regression coefficients (Zhao et al., 2016). TPD Ts values were substituted for TP74 Ts values due to missing data.

Temperature sensitivity (Q_{10}), was calculated as the increasing rate of Rs corresponding to an increase in temperature of 10 °C (as shown in Equation 2):

$$Q_{10} = e^{10b} \tag{2}$$

where *b* is the regression coefficient calculated from Equation 1.

Basal rate of respiration at 10°C (R_{10}) was calculated from Equation 3:

$$R_{10} = ae^{10b} \tag{3}$$

where *a* and *b* are the regression coefficients calculated from Equation 1.

The collected Rs data at both sites were fitted to a model that considers Ts and SM, known as the Rs Ts SM model, given by Equation 4 (Ma and Arian, 2021):

$$Rs = R_{10}Q_{10}^{\frac{Ts-10}{10}} * \left(\frac{1}{1 + e^{a+b*SM}}\right) \tag{4}$$

where *Rs* is the estimated Rs rate, *Ts* is the measured Ts at 5 cm, *SM* is the measured SM at 5 cm and *a* and *b* are regression coefficients calculated from Equation 1. TPD Ts values were substituted for TP74 Ts values. The model parameters are summarized in Table 3.

Ma and Arian (2021) have generated model parameters *a* and *b* along with R_{10} and Q_{10} for 2014 – 2018 at TPD. In addition to the parameters derived for this study, parameters from Ma and Arian (2021) have also been used in some models.

Results

Meteorological Measurements

On average, SM was higher at TPD than at TP74 with the annual average being 0.12 $m^3\ m^{-3}$ at TPD where the annual average for TP74 was 0.11 $m^3\ m^{-3}$. Ta was greater at TPD compared to TP74 in 2021. The mean annual Ta at TPD was 11.26 °C and 10.10 °C at TP74. A direct comparison of Ts at both sites for 2021 is unavailable. However, from January 1st to August 31st, 2021, Ts was warmer at TPD than TP74, with mean 10.04 °C at TPD compared to 9.13 °C at TP74. The mean annual Ts at TPD for 2021 was 10.35°C. Net radiation (Rn) was also consistently higher at TPD than at TP74. Daily maximum Rn at TPD was 244.08 W m^{-2} and 263.32 W m^{-2} at TP74, with both maximums occurring on June 28th. Annual means and extremes are summarized in Table 1.

Environmental Drivers

For the data available in 2021 there was no clear relationship between Rs and Ts or SM at either site. A third-order polynomial was fitted for Rs and for each driver at both sites (Figure 2). The

R^2 values indicated that there was very low correlation between Rs and SM and Rs and Ts at both sites in 2021. TPD Ts vs. Rs did have the best fit compared to the other three plots. As an exponential relationship is expected between Rs and Ts, an exponential function was fitted to the data. The R^2 value between the third-order polynomial and an exponential function was very similar for TPD Ts vs. Rs, however, the third-order polynomial was slightly higher. As site-specific values are important for this analysis, TP39 Ts data was gap filled from September 1st onwards with TP74 Ta values and used for TP74 Ts data.

Rs Trends

For the available data in 2021, total annual Rs at TPD and TP74 were 154.49 and 232.66 g C $m^{-2}year^{-1}$, respectively (Figure 3). However, these values largely underestimated and are not representative of the whole growing season at either site (TPD, n= 77 days, TP74, n=66 days). Most of the data available is from the beginning of August to early October at both sites, with 17 days of additional data available for TPD at the end of November into December. The average daily value was higher at TP74 then TPD (3.55 vs. 3.11 µmol CO2 $m^{-2}s^{-1}$). The lowest daily mean occurred on July 27th at TPD with a value of 0.76 µmol CO2 $m^{-2}s^{-1}$with the highest value at TPD occurring on August 17th with a value of 17.77 µmol CO2 $m^{-2}s^{-1}$. The TP74 the lowest mean daily value was on September 23rd with a value of 2.18 µmol CO2 $m^{-2}s^{-1}$and the largest value of October 3rd with a value of 5.13 µmol CO2 $m^{-2}s^{-1}$, as summarized in Table 2.

During a precipitation event starting the evening of September 7th and continuing into the morning of September 8th, SM rose 197% (0.0345 vs. 0.1025 $m^3 m^{-3}$) at TPD and 31% (0.063 vs. 0.0825 $m^3 m^{-3}$). There was very little change in Rs at TP74 during the SM increase. However, Rs behaved at TPD differed. Hours before the precipitation event there was a rapid decline, before an exponential increase, followed by another rapid decrease, before starting to rise again. This trend is shown in Figure 4.

As seen in Figure 5, on October 3rd, 2021, SM rose at both sites throughout the day with SM peaking at around noon. At TP74, Rs was drastically reduced for the remainder of the day, whereas at TPD, Rs increased throughout the day with the increasing moisture. This trend was also exhibited 11 days earlier on September 22nd. During a period of SM increase, Rs at TP74 gradually reduced throughout the day, whereas Rs at TPD increased in the same time period. Additionally, on September 3rd Rs followed a similar pattern to that described above, but to a lesser degree.

Q_{10} at TPD and TP74 were calculated to be 2.14 and 1.29, respectively. R_{10} at TPD and TP74 were calculated to be 2.34 and 2.96 respectively. Due to available Ts data ending August 31st for TP74, Ts data for TPD was used for the calculations.

Soil respiration modelling

The produced models at TPD and TP74 are shown in Figure 6. At TP74, the model severely underestimated Rs values throughout the year (R^2= 0.19). The estimated sum of Rs for the model was 116.59 g C $m^{-2}year^{-1}$, which is approximately 50% less than the collected Rs data (232.66 g C $m^{-2}year^{-1}$). The poor fit can be explained by the lack of data used to fit the model. Additionally, as Ts is missing for the majority of Rs data points at TP74, Ts data for TPD was substituted for the missing TP74 data to help improve the model. The model produced for TPD was able to perform much better than that of TP74 (R^2= 0.43). However, there were some data points that were underestimated in the model, specifically, late in the year. Overall, the model estimated that the annual sum of Rs is 483.16 g C $m^{2-}year^{-1}$ which is approximately 50% greater than the annual sum of the collected data (157.49 g C $m^{-2}year^{-1}$).

Modelling Rs TPD with past model parameters

Ma and Arain (2021) modelled Rs for the years of 2014 – 2018 at TPD using the same Rs Ts SM model, as above (Equation 4). Additional models were created using 2021 Ts and SM data but the calculated parameters over the five years at TPD (summarized in Table 3) were used instead of the parameters derived in this study. Using the five-year average of the parameters from Ma and Arain (2021) the produced model estimated the annual sum of Rs at TPD to be 1773.2 g C $m^{-2}year^{-1}$, Figure 7. 2021 was the warmest year (11.26 °C) when compared to years within the 2014 – 2018 timeframe. Out of the five years in Ma and Arian's (2021) study, 2016 was the warmest year with the average annual temperature being 10.64 °C. As 2016 had the most similar meteorological year as 2021, Rs for 2021 was modeled using the parameters for 2016. This model estimated that annual Rs at TPD for 2021 was 1169.7 g C $m^{-2}year^{-1}$. Models produced based on the other yearly parameters estimated. Rs at TPD were much higher than the 2016 model, with values from 2017 and 2018 being closer to the average model. Model estimates are summarized in Table 4.

Past model parameters are not available for TP74. As such, no additional models for the conifer site were produced.

Discussion

Rs trends compared between conifer and deciduous forests

Similar patterns of Rs decreasing at TP74 and increasing at TPD with an increase of SM has also been found by Ma (2020). In 2019, Ma (2020) documented that TP74 experienced a decrease of 0.17 µmol CO2 $m^{-2}s^{-1}$ in Rs and TPD experienced an increase of Rs by 1.45 µmol CO2 $m^{-2}s^{-1}$ over the course of the same day when SM was increasing. However, in the previous year, 2018, Ma (2020) reported that after a SM increase of 0.02 and 0.08 m^3 m^{-3} at TP74 and TPD, respectively, Rs increased at both sites by 2.45 µmol CO2 $m^{-2}s^{-1}$and 2.08 µmol CO2 $m^{-2}s^{-1}$.

In a separate precipitation event in 2018, Rs increased at TP74 by 1.32 µmol CO2 $m^{-2}s^{-1}$and at TPD by 1.08 µmol CO2 $m^{-2}s^{-1}$ (Ma, 2020). In both events during the 2018 growing season, the Rs increase was greater at TP74 than TPD, even though SM increased more at TPD than TP74. Daly (2016) has also studied Rs at TPD and also found that Rs increase in response to an increase of SM. In 2014, Daly (2016) reiterated that with a 0.1 m^3 m^{-3} increase of SM at TPD, Rs also increased 5.7 µmol CO2 $m^{-2}s^{-1}$, but Daly did not study TP74.

The typical Rs response to an increase of SM is to increase, as shown at TPD (Orchard and Cook, 1983; Unger et al., 2010; Yan et al., 2014; Liu et al., 2019). Additional examples of Rs declining as a response to increasing SM in conifer forest were not able to be found in the literature, with the typical Rs response of a conifer to increasing SM being documented with the increase. Yuste et al. (2003) showed that in a *Pinus sylvestris L.* forest in a maritime climate, SM was a limiting factor for Rs during the summer and that there were post rainfall increases to Rs.

In a mixed-conifer forest in a Mediterranean climate, Concilio et al. (2009) reported that summer precipitation could cause Rs to temporarily increase, but there was no mention of the decrease pattern at TP74. Similarly, Zheng et al. (2021) found during a four-year study in a mixed temperate forest (dominated by *Quercus variabilis*, *P. tabuliformis*, and *P. orientalis*) a significant increase of Rs after rainfall events, mainly caused by changes in SM. However, the decreasing Rs pattern as seen at TP74 has been observed by Han et al. (2018) in a four-year study of a coastal wetland. Han et al. (2018) demonstrated that the increase of SM reduced daily Rs. Over the course of 3 days, Han et al. (2018) documented a 1.38 µmol CO2 $m^{-2}s^{-1}$in Rs during a precipitation event. Han et al. (2018) propose four different reasons ranging from limited microbial activities to changes in photosynthesis that could play a role in causing the decrease in Rs.

The current study hypothesizes that the organic material content differences might contribute to the Rs declines with increasing SM at TP74. Skopp et al. (1990) showed that with increasing relative water content (RWC), Rs increases until RWC reaches 0.7. Up until 0.7 RWC, the increase in water is increasing diffusion and facilitating the transport of nutrients allowing for increasing values of Rs due to increased productivity of the microbes (Orchard and Cook, 1983; Skopp, Jawson and Doran, 1990; Unger et al., 2010; Yan et al., 2014; Liu et al., 2019). Once RWC is equal to 0.7, Rs begins to decline due to the limitations of oxygen diffusion, which then limits the productivity of the microbes (Skopp et al., 1990). The soil of TP74 contains lower amounts of organic material than at TPD, meaning that porosity will be lower at TP74 than at TPD. As RWC is a function of volumetric water capacity divided by porosity, TP74 will reach higher values of RWC before TPD, explaining why Rs at TP74 is declining while Rs is increasing at TPD. This explanation is within the same vein as one of Han et al. (2018) proposals of the increase of water limiting microbial activities at the site and, therefore, decreasing Rs.

Temperature sensitivity

Q_{10} at TP74 (1.29) is considered to be quite low. In a three-year analysis from 2017 – 2019, Ma (2021) has also found that Q_{10} is lower at TP74. Ma's (2021) mean Q_{10} value for the study years was 1.87, which is 0.58 higher than what was calculated in 2021. The lack of Rs data available would have produced a poor trend. However, conifer forests tend to have lower Q_{10} values. Zhao et al. (2016) studied three conifer and three deciduous forests in a temperate climate. It was found that Q_{10} was 0.55 lower in the conifer forests than in the deciduous forest (1.9 vs. 2.45; Zhao et al., 2016). Therefore, it is reasonable to believe that although 1.29 might be an underestimate of Q_{10} at TP74 for 2021, the true value of Q_{10} is expected to be low.

The 2021 Q_{10} value (2.14) at TPD was also calculated to be lower than the three-year mean (2.49) from Ma (2020). Ma (2020) estimated for 2018 Q_{10} was 2.12, which is lower than 2021. Perhaps with more data available in 2021, Q_{10} would have been calculated to have a higher value at TPD, but with the available data, it is realistic to believe that 2.14 is an accurate value for TPD.

Model Appropriateness

The models that were derived with parameters from the 2021 growing season vastly underestimated Rs at both sites. Rs at TP74 ranged between 647.76 and 777.24 g C m^{-2} $year^{-1}$ from 2017 – 2019. The 2021 model estimated that Rs was 116.59 g C m^{-2} $year^{-1}$ at TP74, which is a clear underestimate based on the past data. Therefore, the 2021 model is not appropriate and should not be used. As no alternative models can be created for TP74, it is unable to be determined what the more appropriate model would be to model the 2021 growing season at this site.

At TPD, the collected Rs data from Ma and Arian's (2021) study ranged from 850.55 g C m^{-2} $year^{-1}$ in 2016 to 1208.94 g C m^{-2} $year^{-1}$ in 2018 (Table 5). When comparing the original 2021 model, which estimates total Rs at TPD was 483.16 g C m^{-2} $year^{-1}$, to the model estimated from Ma and Arian's parameters models, it is clear the 2021 model is not an accurate model for the 2021 growing season. The model with parameters averaged across 2014 – 2018 estimates that Rs was 1773.2 g C m^{-2} $year^{-1}$ for 2021. This model has overestimated Rs compared to past Rs data for the TPD. Therefore, not the ideal model for 2021. The 2016 model, chosen for the similarity in Ta for 2021, suggests that annual Rs was 1169.7 g C m^{-2} $year^{-1}$. The models that were created from the parameters in the other past years all estimated values above the collected data from 2014 – 2018, with the closest value to the range being 2015. With 2016 being the only model within the known range of Rs and best matching Ta for 2021, the 2016 model is the most accurate model for Rs at TPD for 2021.

Rs Ts SM model limitations

The models that were derived for this study poorly fit the data, reiterating the importance of using good observed data when producing models. One of the main contributors to the poor fit is the lack of Rs data available to fit the model. Furthermore, although the fit of Ts at TPD was very close to the values of Ts at TP74, the model for TP74 would have been stronger if using Ts data from the site. As this study has illustrated, the lack of high-quality data is one of the challenges that must be overcome when using Rs models.

Using the TPD models as an example, this study has illustrated that Rs modelling is very reactive to changes with the meteorology and model parameters. As parameters for the Rs Ts SM model are derived from Ts and Rs, the temperature plays an important role in creating an accurate model. Modelling Rs with parameters that were derived for colder years (2014, 2015, 2017 and 2018) resulted in the estimated Rs being higher than what was expected for the site for all years. When choosing a model with parameters that were derived for a year with similar meteorology (2016), the model was able to produce an estimate of Rs that was within the expected range. Additionally, as shown in Figure 8, the average of past years can still result in an overestimation of Rs. Figure 8 also demonstrates how the Rs model can change due to parameters being derived for different meteorology. These results suggest the Rs Ts SM model is highly sensitive to changes in temperature, highlighting the importance of choosing the correct set of parameters for the years' meteorology. Furthermore, using one set of model parameters for a site can produce inaccurate estimations of annual Rs at the site. With this in mind, the accurate use of the Rs Ts SM model to predict Rs is limited to years when previously derived parameters fit the site meteorology closely.

Conclusion

Despite the challenges with data, insight was gained into soil CO_2 movement at both TPD and TP74. The study found that Rs responded differently with an increase of SM between the sites. TP74 often responded to an increase in SM with a decrease of Rs, whereas Rs increased at TPD.

The most probable cause of the discrepancy is due to differences in organic material between the two sites. Further research is needed to confirm what is causing the decrease. This trend demonstrates that not only is Rs strongly influenced by environmental variables but also that there are large differences in Rs between a deciduous and a conifer forest.

Although it fit poorly, Rs Ts SM models were developed for both sites. A more accurate model for TP74 was unable to be produced. However, using past model parameters at TPD from a year with similar Ta, Rs at TPD was estimated to be 1169.7 g C m^{-2} $year^{-1}$. The results of this study illustrate the importance of having good observed data to fit Rs models, and if data is lacking, it is important to choose parameters derived from a year with similar meteorology.

Furthermore, ensuring that future impacts of climate change are understood on Rs is vitally important as Rs is a major component within the global carbon cycle. Continuing to use well-tested models will help to predict Rs and provide insight into future impacts of climate change on CO_2 fluxes from the soil. Overall, this study was able to explore Rs trends and produce Rs models at TPD and TP74, strengthening current knowledge of soil CO_2 fluxes in temperate forests in Southern Ontario.

References

Allen, C.D., Macalady, A.K., Chenchouni, H., Bachelet, D., McDowell, N., Vennetier, M., Kitzberger, T., Rigling, A., Breshears, D.D., Hogg, E.H. (Ted), Gonzalez, P., Fensham, R., Zhang, Z., Castro, J., Demidova, N., Lim, J.-H., Allard, G., Running, S.W., Semerci, A. and Cobb, N., 2010. A global overview of drought and heat-induced tree mortality reveals emerging climate change risks for forests. *Forest Ecology and Management*, 259(4), pp.660–684. https://doi.org/10.1016/j.foreco.2009.09.001.

Beamesderfer, E.R., Arain, M.A., Khomik, M., Brodeur, J.J. and Burns, B.M., 2020. Response of carbon and water fluxes to meteorological and phenological variability in two eastern North American forests of similar age but contrasting species composition – a multiyear comparison. *Biogeosciences*, 17(13), pp.3563–3587. https://doi.org/10.5194/bg-17-3563-2020.

Bhanja, S.N. and Wang, J., 2021. Influence of environmental factors on autotrophic, soil and ecosystem respirations in Canadian boreal forest. *Ecological Indicators*, 125, p.107517. https://doi.org/10.1016/j.ecolind.2021.107517.

Bonan, G.B., 2008. Forests and Climate Change: Forcings, Feedbacks, and the Climate Benefits of Forests. *Science*, 320(5882), pp.1444–1449. https://doi.org/10.1126/science.1155121.

Bond-Lamberty, B., Bailey, V.L., Chen, M., Gough, C.M. and Vargas, R., 2018. Globally rising soil heterotrophic respiration over recent decades. *Nature*, 560(7716), pp.80–83. https://doi.org/10.1038/s41586-018-0358-x.

Borken, W., Xu, Y.-J., Davidson, E.A. and Beese, F., 2002. Site and temporal variation of soil respiration in European beech, Norway spruce, and Scots pine forests. *Global Change Biology*, 8(12), pp.1205–1216. https://doi.org/10.1046/j.1365-2486.2002.00547.x.

Bradford, M.A., Wieder, W.R., Bonan, G.B., Fierer, N., Raymond, P.A. and Crowther, T.W., 2016. Managing uncertainty in soil carbon feedbacks to climate change. *Nature Climate Change*, 6(8), pp.751–758. https://doi.org/10.1038/nclimate3071.

Concilio, A., Chen, J., Ma, S. and North, M., 2009. Precipitation drives interannual variation in summer soil respiration in a Mediterranean-climate, mixed-conifer forest. *Climatic Change*, 92(1), pp.109–122. https://doi.org/10.1007/s10584-008-9475-0.

Daly, K., 2016. *An Analysis of Soil Respiration in a Temperate Deciduous Forest Ecosystem*. [Thesis] Available at: <https://macsphere.mcmaster.ca/handle/11375/19143> [Accessed 28 September 2021].

Giasson, M.-A., Ellison, A.M., Bowden, R.D., Crill, P.M., Davidson, E.A., Drake, J.E., Frey, S.D., Hadley, J.L., Lavine, M., Melillo, J.M., Munger, J.W., Nadelhoffer, K.J., Nicoll, L., Ollinger, S.V., Savage, K.E., Steudler, P.A., Tang, J., Varner, R.K., Wofsy, S.C., Foster, D.R. and Finzi, A.C., 2013. Soil respiration in a northeastern US temperate forest: a 22-year synthesis. *Ecosphere*, 4(11), p.art140. https://doi.org/10.1890/ES13.00183.1.

Han, G., Sun, B., Chu, X., Xing, Q., Song, W. and Xia, J., 2018. Precipitation events reduce soil respiration in a coastal wetland based on four-year continuous field measurements. *Agricultural and Forest Meteorology*, 256–257, pp.292–303. https://doi.org/10.1016/j.agrformet.2018.03.018.

Hibbard, K.A., Law, B.E., Reichstein, M. and Sulzman, J., 2005. An analysis of soil respiration across northern hemisphere temperate ecosystems. *Biogeochemistry*, 73(1), pp.29–70. https://doi.org/10.1007/s10533-004-2946-0.

Huang, N., Gu, L. and Niu, Z., 2014. Estimating soil respiration using spatial data products: A case study in a deciduous broadleaf forest in the Midwest USA. *Journal of Geophysical Research: Atmospheres*, 119(11), pp.6393–6408. https://doi.org/10.1002/2013JD020515.

Johnston, A.S.A. and Sibly, R.M., 2018. The influence of soil communities on the temperature sensitivity of soil respiration. *Nature Ecology & Evolution*, 2(10), pp.1597–1602. https://doi.org/10.1038/s41559-018-0648-6.

Klimek, B., Chodak, M. and Niklińska, M., 2021. Soil respiration in seven types of temperate forests exhibits similar temperature sensitivity. *Journal of Soils and Sediments*, 21(1), pp.338–345. https://doi.org/10.1007/s11368-020-02785-y.

Lei, J., Guo, X., Zeng, Y., Zhou, J., Gao, Q. and Yang, Y., 2021. Temporal changes in global soil respiration since 1987. *Nature Communications*, 12(1), p.403. https://doi.org/10.1038/s41467-020-20616-z.

Liu, Y., Liu, S., Miao, R., Liu, Y., Wang, D. and Zhao, C., 2019. Seasonal variations in the response of soil CO2 efflux to precipitation pulse under mild drought in a temperate oak (Quercus variabilis) forest. *Agricultural and Forest Meteorology*, 271, pp.240–250. https://doi.org/10.1016/j.agrformet.2019.03.009.

Ma, Y. and Arain, M.A., 2021. *Evaluating environmental controls on soil respiration in a deciduous forest in the Great Lakes region using various modeling approaches*. [Unpublished manuscript] School of Earth, Environment and Society and McMaster Centre for Climate Change, McMaster University.

Ma, Y., 2020. *Analysis and Modelling of Soil CO2 Emissions Within Temperate Coniferous and Deciduous Forests*. [Thesis] Available at: <https://macsphere.mcmaster.ca/handle/11375/26010> [Accessed 13 March 2022].

Orchard, V.A. and Cook, F.J., 1983. Relationship between soil respiration and soil moisture. *Soil Biology and Biochemistry*, 15(4), pp.447–453. https://doi.org/10.1016/0038-0717(83)90010-X.

Piao, S., Luyssaert, S., Ciais, P., Janssens, I.A., Chen, A., Cao, C., Fang, J., Friedlingstein, P., Luo, Y. and Wang, S., 2010. Forest annual carbon cost: a global-scale analysis of autotrophic respiration. *Ecology*, 91(3), pp.652–661. https://doi.org/10.1890/08-2176.1.

Ryan, M.G., 1991. Effects of Climate Change on Plant Respiration. *Ecological Applications*, 1(2), pp.157–167. https://doi.org/10.2307/1941808.

Skopp, J., Jawson, M.D. and Doran, J.W., 1990. Steady-State Aerobic Microbial Activity as a Function of Soil Water Content. *Soil Science Society of America Journal*, 54(6), pp.1619–1625. https://doi.org/10.2136/sssaj1990.03615995005400060018x.

Smith, A.P., Bond-Lamberty, B., Benscoter, B.W., Tfaily, M.M., Hinkle, C.R., Liu, C. and Bailey, V.L., 2017. Shifts in pore connectivity from precipitation versus groundwater rewetting increases soil carbon loss after drought. *Nature Communications*, 8(1), p.1335. https://doi.org/10.1038/s41467-017-01320-x.

Song, B., Niu, S. and Wan, S., 2016. Precipitation regulates plant gas exchange and its long-term response to climate change in a temperate grassland. *Journal of Plant Ecology*, 9(5), pp.531–541. https://doi.org/10.1093/jpe/rtw010.

Tang, X., Du, J., Shi, Y., Lei, N., Chen, G., Cao, L. and Pei, X., 2020. Global patterns of soil heterotrophic respiration – A meta-analysis of available dataset. *CATENA*, 191, p.104574. https://doi.org/10.1016/j.catena.2020.104574.

Teskey, R., Wertin, T., Bauweraerts, I., Ameye, M., Mcguire, M.A. and Steppe, K., 2015. Responses of tree species to heat waves and extreme heat events. *Plant, Cell & Environment*, 38(9), pp.1699–1712. https://doi.org/10.1111/pce.12417.

Unger, S., Máguas, C., Pereira, J.S., David, T.S. and Werner, C., 2010. The influence of precipitation pulses on soil respiration – Assessing the “Birch effect” by stable carbon isotopes. *Soil Biology and Biochemistry*, 42(10), pp.1800–1810. https://doi.org/10.1016/j.soilbio.2010.06.019.

Wei, W., Weile, C. and Shaopeng, W., 2010. Forest soil respiration and its heterotrophic and autotrophic components: Global patterns and responses to temperature and precipitation. *Soil Biology and Biochemistry*, 42(8), pp.1236–1244. https://doi.org/10.1016/j.soilbio.2010.04.013.

Yan, L., Chen, S., Xia, J. and Luo, Y., 2014. Precipitation Regime Shift Enhanced the Rain Pulse Effect on Soil Respiration in a Semi-Arid Steppe. *PLOS ONE*, 9(8), p.e104217. https://doi.org/10.1371/journal.pone.0104217.

Yuste, J.C., Janssens, I.A., Carrara, A., Meiresonne, L. and Ceulemans, R., 2003. Interactive effects of temperature and precipitation on soil respiration in a temperate maritime pine forest. *Tree Physiology*, 23(18), pp.1263–1270. https://doi.org/10.1093/treephys/23.18.1263.

Yuste, J.C., Nagy, M., Janssens, I.A., Carrara, A. and Ceulemans, R., 2005. Soil respiration in a mixed temperate forest and its contribution to total ecosystem respiration. *Tree Physiology*, 25(5), pp.609–619. https://doi.org/10.1093/treephys/25.5.609.

Zhao, X., Li, F., Zhang, W., Ai, Z., Shen, H., Liu, X., Cao, J. and Manevski, K., 2016. Soil Respiration at Different Stand Ages (5, 10, and 20/30 Years) in Coniferous (Pinus tabulaeformis Carrière) and Deciduous (Populus davidiana Dode) Plantations in a Sandstorm Source Area. *Forests*, 7(8), p.153. https://doi.org/10.3390/f7080153.

Zheng, P., Wang, D., Yu, X., Jia, G., Liu, Z., Wang, Y. and Zhang, Y., 2021. Effects of drought and rainfall events on soil autotrophic respiration and heterotrophic respiration. *Agriculture, Ecosystems & Environment*, 308, p.107267. https://doi.org/10.1016/j.agee.2020.107267.

Tables

Table 1.1: Mean, minimum and maximum values of soil moisture (SM), air temperature (Ta), soil temperature at 5 cm (Ts), and net radiation at TPD from January 1st to December 31st, 2021.

TPD				
	SM ($m^3 m^{-3}$)	Ta (°C)	Ts_5cm (°C)	Rn (Wm^{-2})
Mean	0.12	11.26	10.35	NA
Min	0.03	-11.05	-0.6	-19.65
Max	0.22	26.89	22.45	244.08

Table 2.2: Mean, minimum and maximum values of soil moisture (SM), air temperature (Ta), and net radiation at TP74 from January 1st to December 31st, 2021. Soil temperature at 5 cm (Ts) data values are from January 1st to August 31st, 2021, due to equipment malfunction.

TP74				
	SM ($m^3 m^{-3}$)	Ta (°C)	Ts_5cm (°C)	Rn (Wm^{-2})
Mean	0.11	10.1	9.13	NA
Min	0.06	-15.13	-1.89	-35.12
Max	0.21	30.8	21.82	263.32

Table 3: The minimum recorded daily mean of soil respiration, and maximum recorded daily mean of soil respiration from July to December 2021, at TPD and TP74.

	Minimum Daily Mean		Maximum Daily Mean	
	Date	Value (μmol $CO2\ m^{-2}s^{-1}$)	Date	Value (μmol $CO2\ m^{-2}s^{-1}$)
TPD	27-Jul	0.76	17-Aug	17.77
TP74	23-Sep	2.18	03-Oct	5.13

Table 4: Annual mean Ta in °C followed by the regression coefficients used in the Rs Ts SM model calculated from Equation 1 at both sites. After the table brake, 2021 Rs Sum is the annual estimate of soil respiration in g C m^{-2} $year^{-1}$ as calculated by the respective model. The r^2 value for both models are also included.

	Mean Ta (°C)	*a*	*b*	Q_{10}	R_{10}		2021 Rs Sum (g C m^{-2} $year^{-1}$)	r^2
TPD	11.26	1.091	0.06304	2.14	2.34		483.16	0.43
TP74	10.1	2.291	0.02339	1.29	2.96		116.59	0.19

Table 5: Annual mean Ta in °C followed by the regression coefficients found in Ma and Arian (2020) for TPD. After the table brake, 2021 Rs Sum is the annual estimate of soil respiration in g C m^{-2} $year^{-1}$ as calculated by the respective model. The r^2 value for the models are also included.

	Mean Ta (°C)	*a*	*b*	Q_{10}	R_{10}		2021 Rs Sum (g C m^{-2} $year^{-1}$)	r^2
2014	7.93	1.17	-17.67	2.51	6.07		1938.2	0.4523
2015	9.04	0.89	-17.55	2.32	3.87		1281.3	0.4643
2016	10.64	1.46	-87.91	2.03	2.77		1169.7	0.4761
2017	9.93	0.9	-63.23	1.89	4.3		1747.8	0.4852
2018	9.22	0.029	-18.65	2.76	3.97		1706.6	0.4862
Mean	9.35	0.8898	-41.002	2.302	4.196		1773.2	0.4954

Table 6: Annual measures soil respiration at TPD in µmol CO2 $m^{-2}s^{-1}$ from 2014 – 2018. Data is from Ma and Arian (2021).

	Measured Rs (µmol CO2 $m^{-2}s^{-1}$)
2014	906.19
2015	894.61
2016	850.55
2017	1162.87
2018	1208.94
Mean	1004.632

Figures

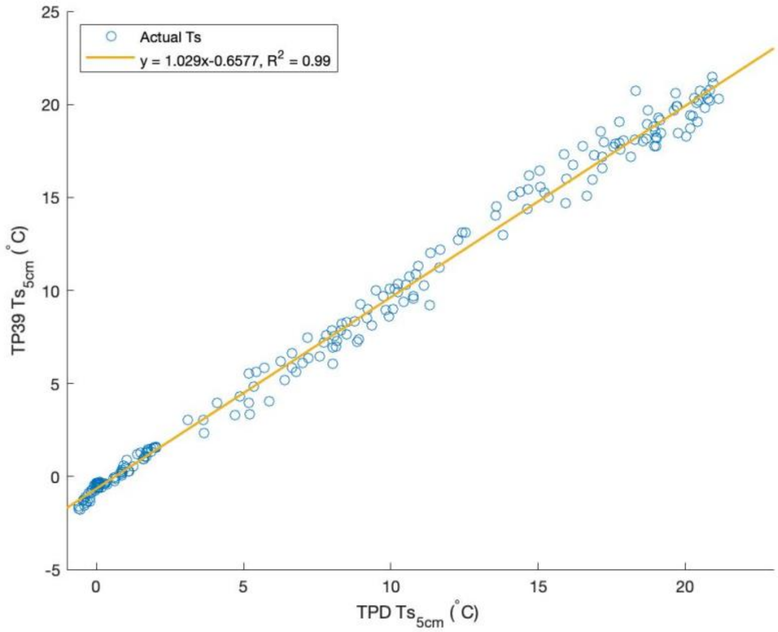

Figure 1: The relationship between soil temperature (Ts) at 5 cm at TPD vs. TP39, until August 31st, 2021. Blue circles are the measured values, and the yellow line is the line of best fit (y=1.029x-0.6577), R^2=0.99.

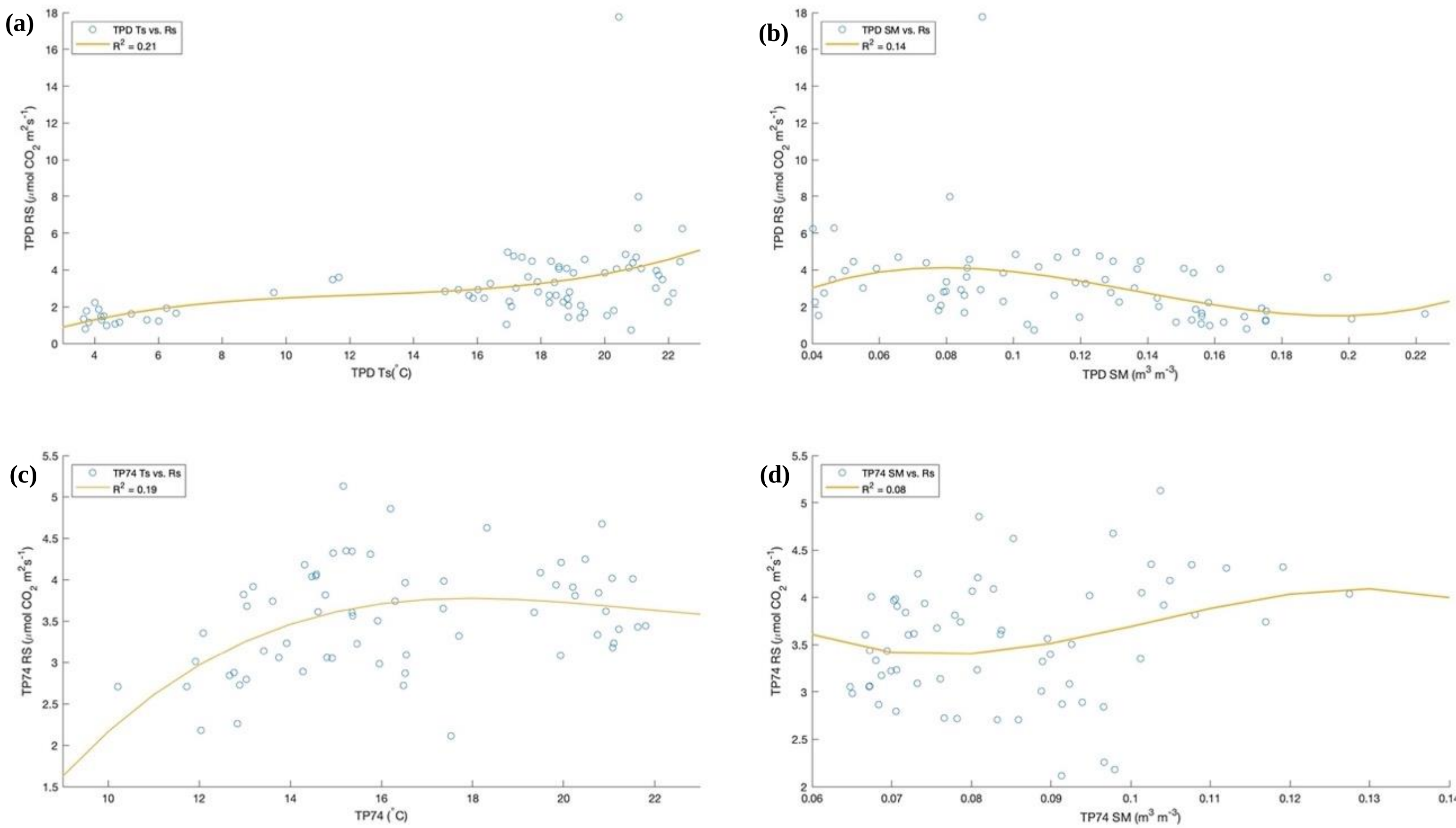

Figure 2: The relationship between soil respiration (Rs) and soil temperature (Ts) and soil moisture (SM) at TPD is shown in a and b, respectively. The relationship between soil respiration (Rs) and soil temperature (Ts) and soil moisture (SM) at TP74 is shown in c and d, respectively. Blue circles are the measured values, and the yellow line is the line of best fit, all are third-order polynomials. R^2 values are included in the legend.

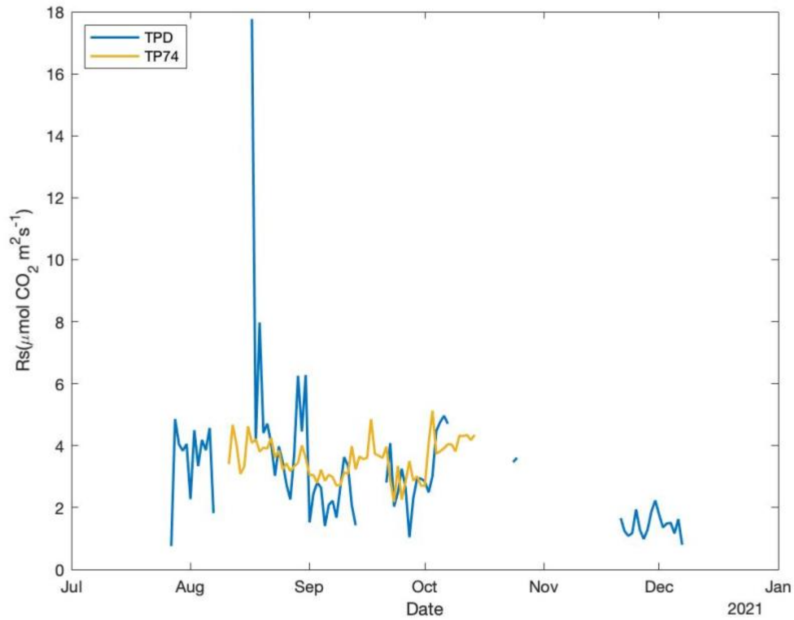

Figure 3: Daily mean of soil respiration (Rs) at TPD (blue) and TP74 (yellow) over the 2021 growing season. Due to equipment malfunction, data is only available for 77 days between July 27th to December 7th, 2021, at TPD. At TP74, 66 days of data are available between August 5th and October 10th, 2021.

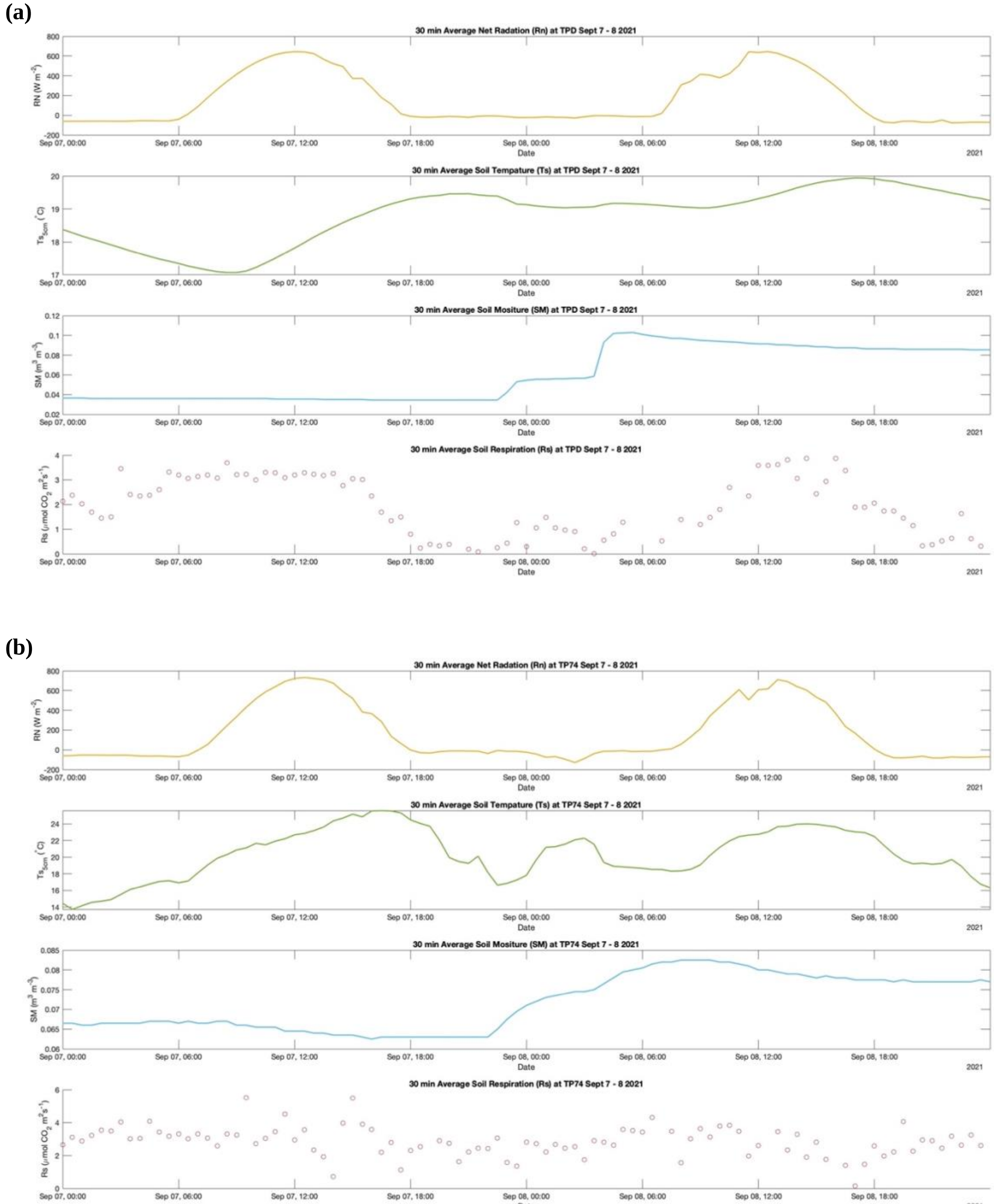

Figure 4: Net radiation (Rn; yellow), temperature (soil temperature (Ts) at TPD, air temperature (Ta) at TP74; green), soil moisture (SM; blue) and soil respiration (Rs; red) at TPD (a) and TP74 (b) from September 7th to 8th. During an increase of SM at both sites, very little change of Rs at occurred at TP74. However, at TPD, hours before the precipitation event there was a rapid decline, before and exponential increase, followed by another rapid decrease, before starting to rise again.

(a)

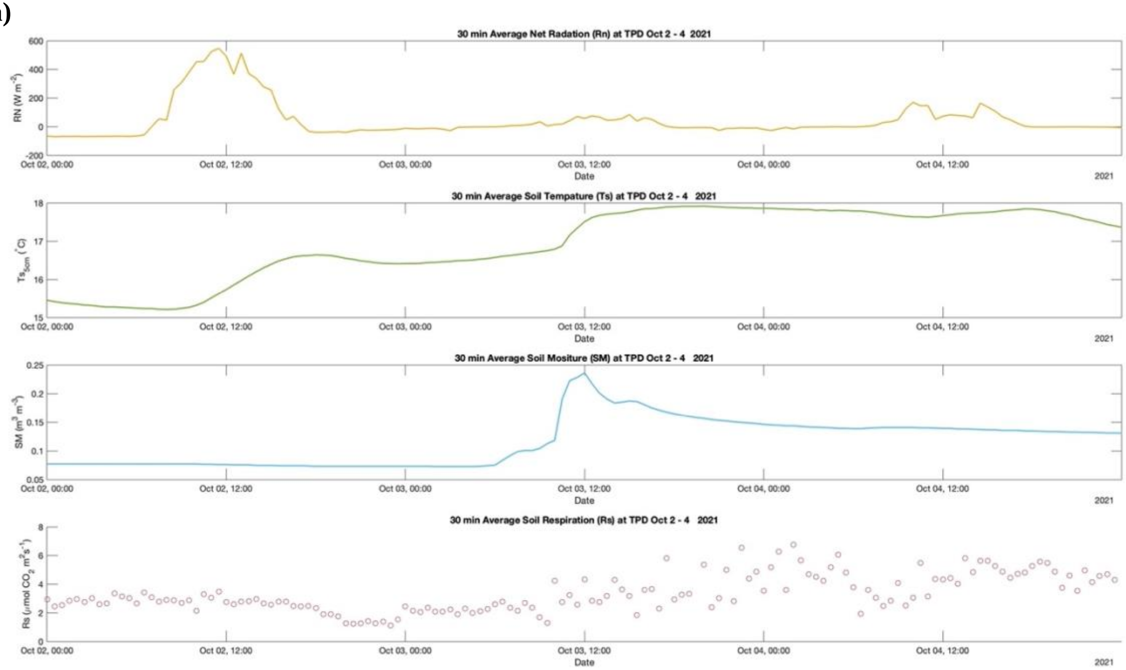

(b)

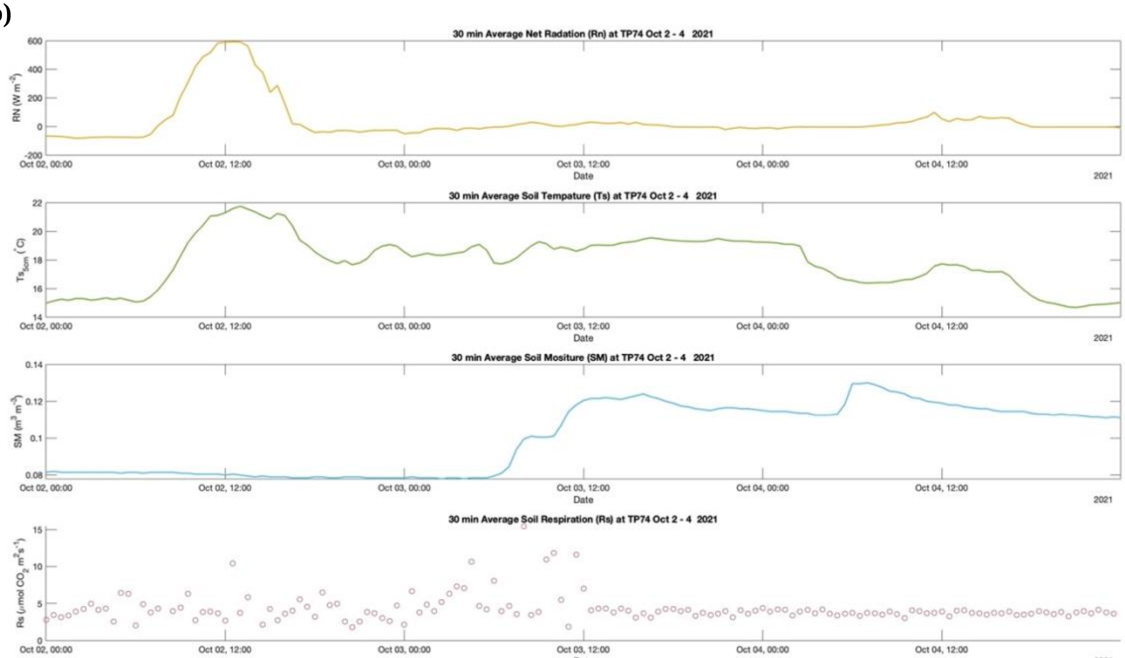

Figure 5: Net radiation (Rn; yellow), temperature (soil temperature (Ts) at TPD, air temperature (Ta) at TP74; green), soil moisture (SM; blue) and soil respiration (Rs; red) at TPD (a) and TP74 (b) from October 2nd to 4th. During an increase of SM at both sites, Rs at TPD increased whereas Rs decreased at TP74.

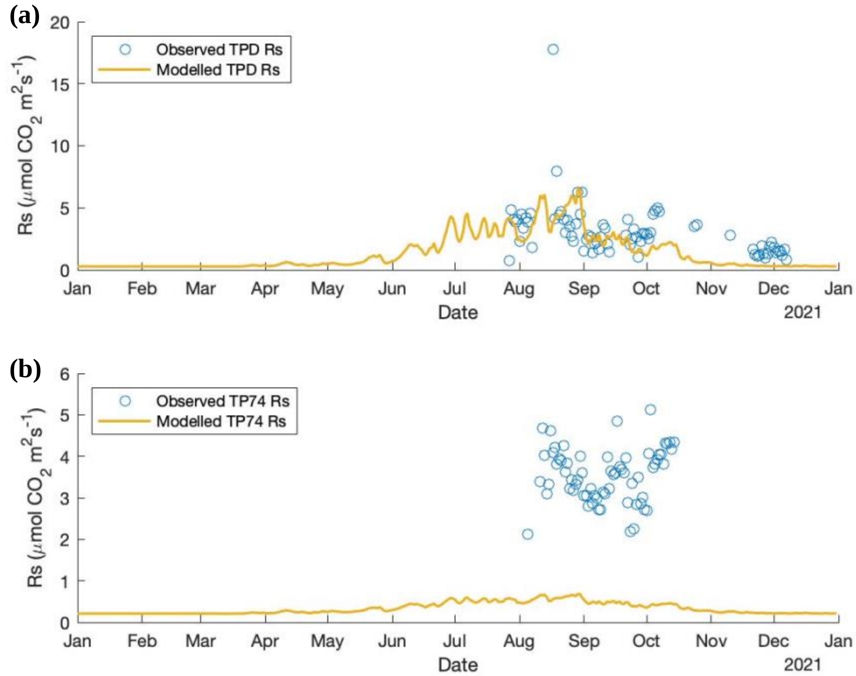

Figure 6: Annual observed soil respiration (Rs) values compared to the estimated soil respiration (Rs) values for 2021 at TPD (a) and TP74 (b). Blue circles are the measured values, and the yellow line is the predicted values from the Rs Ts SM model.

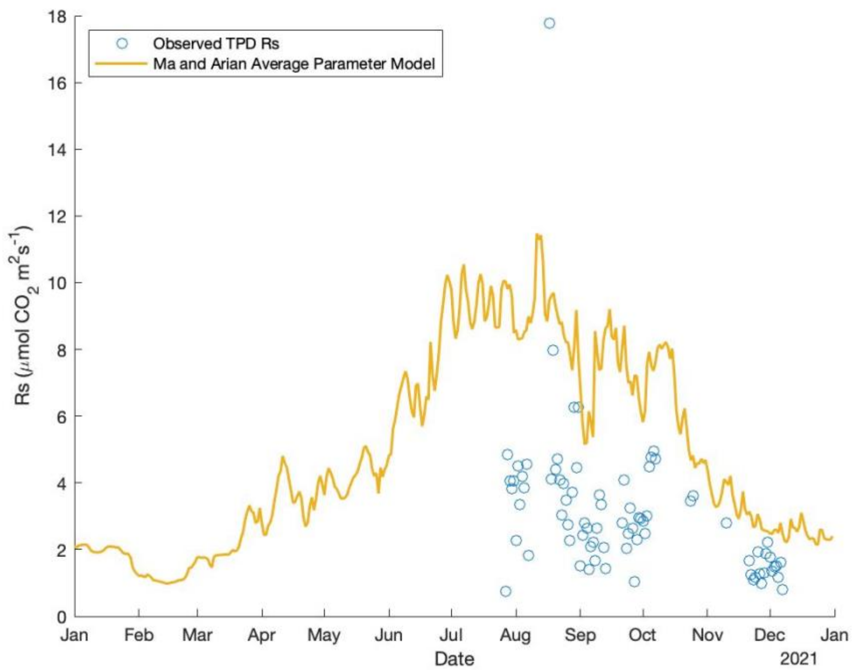

Figure 7: Annual observed soil respiration (Rs) values, compared to the estimated soil respiration (Rs) values, for 2021 at TPD. Model used is the Rs Ts SM model using average parameters from 2014 – 2018 Ma and Arian's (2021). Blue circles are the measured values, and the yellow line is the predicted values.

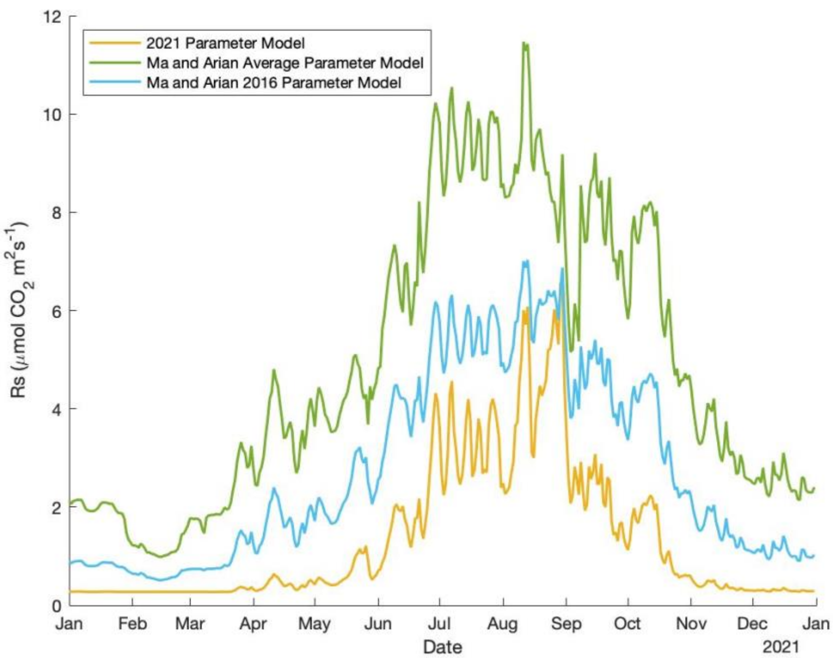

Figure 8: Comparison of Rs Ts SM model using three different parameter sets for TPD for 2021. The yellow line is the estimated soil respiration (Rs) using parameters derived in this study. The green line is the same model but using average values of parameters from 2014 to 2018. Parameters were derived for TPD. The blue line is the same model, but parameters are from 2016, which is the closest meteorological match for available model parameters. See Table 3 and 4 for parameter values.